DEVELOPMENT OF 3-D OPTIMIZED PERIMETER ARRAYS FOR NEAR SURFACE GEOPHYSICAL SURVEY USING MODIFIED COMPARE-R METHOD

FATHI MOHAMMED SAEED ABDULLAH

UNIVERSITI SAINS MALAYSIA

2019

DEVELOPMENT OF 3-D OPTIMIZED PERIMETER ARRAYS FOR NEAR SURFACE GEOPHYSICAL SURVEY USING MODIFIED COMPARE-R METHOD

by

FATHI MOHAMMED SAEED ABDULLAH

Thesis submitted in fulfilment of the requirements
for the degree of
Doctor of Philosophy

June 2019

ACKNOWLEDGEMENT

First and foremost, Praise and thank Almighty Allah for bestowing good health, knowledge and for giving me this great opportunity to pursue a doctoral degree.

I would like to express my profound gratitude to my supervisor, Prof. Dr. Mohd Nawawi, for his guidance, encouragement and helpful throughout the period of my research. Without his generous and indispensable help, the conduct of the Ph.D. would not have been possible. I would also like to express my thanks to my Co-supervisor, Prof. Dr. Khiruddin Abdullah for his timely and effective guidance at the early stage of my work.

Special thanks go to my field supervisor Dr. Loke Meng Heng (Geotomo Software Sdn Bhd) for helping me to understand this new topic and generating the optimized arrays. I am greatly indebted for his invaluable discussion throughout the progress of this dissertation and his precious comments contributed enormously to the production of my thesis. I would like to thank Dr. A. Tejero- Andrade (Universidad Nacional Auto´noma de Me´xico) for supplying a copy of the ‘‘L and Corner’’ arrays measurement sequences.

I would also express my heartfelt thanks to Dr. Amin Esmail Khalil, for his moral support, encouragement, and who offered me much advice for my general life and future research works and always he was with me whenever I needed him.

I wish to thank Dr. Tarek Arafa Hamed (National Research Institute of Astronomy and Geophysics (NRIAG), Egypt), for his significant discussion about the principles and theory of resistivity and Magnetotelluric methods throughout our field trip in March 2016 at Ulu-Slim area. I also appreciate the support I received from Dr. Mohd Hariri Arifin (Geo Resources Technology Sdn Bhd), who gives me a chance to

do a 3-D fieldwork using his resistivity meter SAS4000 in Kampar area, Perak. I appreciate the effort and help I received from Dr. Ismail Ahmad Abir.

I wish to thank the staff and postgraduate students in the school of physics for their friendship and cooperation. Special thanks go to Mr. Azmi Abdullah, Zulkeflee Ismail, and Yaakob Othman for their help during the field works. In a special case, my deep thanks go to Nuraddin Usman, Arisona Arisona, Mohd Hanis and Geraldine Anukwu for being very helping and cooperative.

I acknowledge the inspiration and encouragement provided by my family members. The memory of my father, may Allah reward him with Jannatul Firdaus. My mother, she always encourages and inspires me in pursuing my Ph.D. I would also like to convey my heartfelt thanks to my beloved elder brothers Abdulhakeem, Gharsan, and Hamoud without their support I would have never achieved this dream and the assistance I received from them throughout my life stages will never be forgotten.

I highly appreciate, and I remain indebted to my lovely wife and children (Rawah, Elyas, and Aleen) for their understanding and patience to stay away from them during the progress of this work.

I gratefully acknowledge the financial support of Taiz University, Yemen for granting me a chance to continue my postgraduate study and my deep thanks to USM, which provided me with all the facilities through my study.

TABLE OF CONTENTS

LIST OF TABLES

Page

LIST OF FIGURES

Page

LIST OF ABBREVIATIONS

1-D	One dimensional
2-D	Two dimensional
3-D	Three dimensional
A-B	Current electrode pair
BGS	British Geological Survey
BGS-CR	British Geological Survey-Compare R
CMPCC	Common Mid-Point Cross-Correlation
CR	Compare R
CPU	Central Processing Unit
DC	Direct Current
DD	Dipole-Dipole
DRAM	Dynamic random-access memory
ERT	Earth Resistivity Tomography
EQ	Equatorial-dipole
ETH	Eidgenossische Technische Hochschule (Goodness Function Method)
GF	Goodness Function
GPU	Graphic Processing Unit
IP	Induced polarization

MAE	Mean Absolute Error
MAPE	Mean Absolute Percentage Error
MASW	Multichannel Analysis of Surface Waves
MC	Minimum-coupling
MGF	Modified Goodness Function
M-N	Potential Electrode Pair
NERC	Natural Environment Research Council
NWCR	Noise-weighted Compare R
NWOPN6	Noise-weighted optimized perimeter arrays with n=6
NWOPN10	Noise-weighted optimized perimeter arrays with n=10
OPN6	Optimized perimeter arrays with n=6
OPN10	Optimized perimeter arrays with n=10
P	Potential
PC	Personal Computer
PCC	Pearson Correlation Coefficient
PD	Pole-Dipole array
PP	Pole-Pole array
R	Model Resolution Matrix
RES2DMOD	Resistivity 2-D Modelling software
RES2DINV	Resistivity 2-D Inversion software

RES3DMOD	Resistivity 3-D Modelling software
RES3DINV	Resistivity 3-D Inversion software
RMS	Root Mean Square
SAS 4000	Signal Averaging System 4000
SSE	Streaming SIMD Extensions
SP	Self-Potential
USM	Universiti Sains Malaysia
W	Wenner array
WS	Wenner-Schlumberger array

LIST OF SYMBOLS

A	Area cross section
a	Electrode spacing
C	Constrained matrix
C_1	Current electrode No.1
C_2	Current electrode No.2
W(*f*)	Weighting function
cm	Centimetre
E	Electrical field intensity
F_{CR}	Ranking function
G	Jacobian matrix
I	Current
J	Current density
K	Geometric factor
K_C	Characteristic geometric factor
K_{max}	Maximum geometric factor
M	Electrode array combination
m	Meter
M_P	Misfit Parameter
msec	Millisecond

mv	Millivolt
N	Electrode number
n	Dipole spacing (The ration of the distance between C1 and P1 or (C2-P2) and the distance between potential electrodes (P1-P2)
na	The spacing between the innermost electrode pair
P_1	Potential electrode No. 1
P_2	Potential electrode No. 2
R_{b+1}	Resolution matrix of the base set plus new array
R_C	Resolution of the comprehensive set
R_r	Relative model resolution
r	The radial distance from the current electrode
$S_m(j)$	The distance of the cell centre from the nearest electrode
S_{max}	Maximum distance of any interior cell from the electrode
V_S	Shear wave velocity
W_d	The square root of the priori data covariance matrix
$\Delta\phi$	potential difference
λ	Damping factor
ρ	resistivity
ΔR_b	Change in the model resolution of the base dataset
ρ_a	Apparent resistivity
ϕ	Electric potential

$-\nabla\phi$	Negative gradient of the electric potential (ϕ)
$\nabla.\mathrm{J}$	The divergence of the current density
$\nabla^2\emptyset$	∇^2 is a second derivative operator and $\emptyset$ is the potential
σ_E	The electrical conductivity of the medium
ρ_i	Inverted resistivity
ρ_t	True resistivity
ε	Constant level error

PEMBANGUNAN SUSUN ATUR PERIMETER 3-D YANG DIOPTIMUMKAN UNTUK SURVEI GEOFIZIK DEKAT PERMUKAAN MENGGUNAKAN KAEDAH UBAHSUAI "COMPARE-R"

ABSTRAK

Mengikut pengimejan kerintangan bumi, pemerolehan data lapangan dan susunan elektrod adalah aspek yang penting untuk dipertimbangkan bagi memastikan kualiti data dan resolusi model yang mantap. Terdapat banyak tatarajah konvensional dengan geometri yang berbeza yang digunakan untuk survei kerintangan dan masing-masing mempunyai prestasi yang berbeza. Baru-baru ini, terdapat trend baru dalam pemerolehan data kerintangan iaitu tatarajah yang dioptimumkan yang telah dibangunkan untuk menambah baik resolusi model subpermukaan. Kajian ini memberi tumpuan kepada penggunaan, penambahbaikan dan penilaian terhadap tatarajah yang dioptimumkan berdasarkan kaedah 'Compare R' yang diubahsuai untuk survei kerintangan 2-D dan mengubahsuaikan nya untuk bersesuaian dengan kes khas survei kerintangan 3-D (kawasan yang terbatas). Dalam survei kerintangan 2-D, keberkesanan dan prestasi tatarajah yang dioptimumkan mengguna kaedah 'Noise-Weighted Compare R' (NWCR) dan kaedah 'Compare R' (CR) dinilai dari segi peningkatan resolusi model subpermukaan dan menyelesaikan sasaran subpermukaan. Keberkesanan tatarajah yang dioptimumkan ini dibandingkan dengan tatarajah konvensional yang biasa digunakan iaitu Dipole-Dipole (DD), Wenner-Schlumberger (WS) dan Wenner (W). Perbandingan ini ditunjukkan mengikut tiga tahap yang berbeza merangkumi ujian model sintetik, uji kaji makmal dan kajian kes lapangan. Prestasi dan ketepatan hasil penyongsangan telah dinilai di tahap pemodelan sintetik menggunakan siri parameter statistik. Walau bagaimanapun, dalam kajian kes

lapangan, pengesahan dijalankan menggunakan sumber maklumat tambahan seperti kaedah geofizik lain atau rekod litologi dari lubang gerudi yang tersedia. Hasilnya menunjukkan bahawa kedua-dua tatarajah yang dioptimumkan menghasilkan resolusi yang lebih baik dan pengesanan sasaran subpermukaan yang lebih tepat khususnya di bahagian paling dalam bagi imej penyongsangan berbanding tatarajah konvensional. Walau bagaimanapun, terdapat sedikit peningkatan NWCR dari segi ketiadaan data yang lebih rendah dan pengesanan sasaran yang lebih baik daripada tatarajah lain. Secara umum, tatarajah yang dioptimumkan adalah berfaedah dalam menghasilkan taburan kerintangan subpermukaan yang lebih realistik. Di samping itu, penyelidikan ini juga diperluaskan untuk mengubah suai algoritma 'Compare R' bagi menghasilkan susunan elektrod secara automatik di mana resolusi model dimaksimumkan untuk pengukuran kerintangan yang terhad kepada perimeter kawasan yang dikaji (survei 3-D). Pembaikan baru bagi tatarajah ini untuk kes penambahan pemberat hingar kepada algoritma (perimeter susunan yang dioptimumkan dan ditambah pemberat hingar) diperkenalkan dan dinilai. Oleh itu, prestasi susunan perimeter yang optimum digambarkan dan dibandingkan dengan tatasusunan L dan 'Corner' standard yang terkini dibangunkan untuk mengatasi masalah berkaitan kawasan yang terbatas. Prestasi telah nilai mengikut tiga tahap: ujian resolusi model, ujian pemodelan sintetik dan kajian kes bidang. Keputusan menunjukkan keupayaan berpotensi bagi tatasusunan perimeter yang optimum untuk menyiasat dan mengatasi keadaan geologi yang mencabar di kawasan yang terbatas (persekitaran bandar) dengan resolusi model yang baik dan penyelidikan yang lebih mendalam.

DEVELOPMENT OF 3-D OPTIMIZED PERIMETER ARRAYS FOR NEAR SURFACE GEOPHYSICAL SURVEY USING MODIFIED COMPARE-R METHOD

ABSTRACT

In earth resistivity imaging, the field data acquisition and the electrodes arrangement are significant aspects to consider for ensuring the highest data quality and highest model resolution. There are many conventional arrays with different geometries used for resistivity surveys and each of them has different performances. Recently, there is a new trend in resistivity data acquisition, which is optimized arrays that developed to improve the subsurface model resolution. This research focused on applying, improving and evaluating the optimized arrays based on a modified compare R method for 2-D resistivity surveys and its modification for the special case of 3-D resistivity surveys (constrained areas). In the 2-D resistivity surveys, the effectiveness and performance of the noise-weighted compare R (NWCR) and compare R (CR) optimized arrays were evaluated in terms of improving the subsurface model resolution and detectability of the near surface targets. The effectiveness of these optimized arrays was compared with commonly used conventional arrays, namely Dipole-Dipole (DD), Wenner-Schlumberger (WS) and Wenner (W). This is demonstrated in three different stages containing synthetic model tests, laboratory experiment and field cases studies. The results show that both optimized arrays perform better resolution and better detectability of the near surface targets especially in the deepest part of the inversion images than conventional arrays. However, there is a slight improvement of NWCR in terms of lower data misfit and better targets detectability than other arrays. Therefore, optimized arrays are advantageous in

creating a more realistic subsurface resistivity distribution. In addition, this research was also extended to introduce and evaluate the modified ‘Compare R’ algorithm to automatically generate electrode arrays that maximize the model resolution for resistivity measurements constrained to the perimeter of a surveyed area (3-D survey). The improvement of these arrays in case of adding the noise-weighted to the algorithm (noise-weighted optimized perimeter arrays) was also introduced and evaluated. Therefore, the performance of four sets of optimized perimeter arrays was illustrated and compared with the standard ‘L and Corner’ (LC) arrays that are developed up-to-date to overcome the constrained areas. The performances were examined using synthetic modelling test and field cases studies. The results show the good capability of the optimized perimeter arrays to investigate and overcome the challenging geologic conditions in the constrained area (urban environment) with good model resolution and deeper investigations.

CHAPTER 1

INTRODUCTION

1.1 Overview

This chapter describes the general overview associated with the resistivity method and the significance of the research undertaken in improving the performance of the earth resistivity tomography to detect and characterize subsurface structures. Brief outlines of the work that has been conducted to date concerning the Compare R (CR) optimized array methods and their limitations are provided. It outlines the motivation; problem statement and research objectives. Finally, an overview of the thesis layout is presented.

In resistivity techniques, most of the conventional resistivity arrays have some disadvantages such as low resolution, low horizontal and vertical coverage, low signal strength, and shallow penetration depth (Loke, 2016 and 2018). Recently, the application of direct current (DC) resistivity method for addressing a wide variety of geological, environmental, engineering, hydrogeological, geothermal issues has increased. This is because of the availability of accurate forward modelling and inversion schemes for both 2-D and 3-D datasets and capabilities of multi-electrode data acquisition systems to select any electrodes configurations. The increasing popularity of DC resistivity imaging has resulted in an increasing demand for the more effective design of resistivity surveys. The improvements in collecting high quality data and maximizing the subsurface model resolution become an attractive research area. In this regards, new algorithms techniques have been introduced into automatically select non-conventional electrode configurations that produce a more

realistic subsurface resistivity distribution (Loke et al., 2010a; Maurer et al., 2010; Stummer et al., 2004; Wilkinson et al., 2006a, 2012).

Recently, there had been significant progress in the automatic techniques to uncover the optimum set of electrode configurations, and increasing the resolution of the subsurface structural imaging for applications where conventional methods are inadequate (Loke et al., 2010a; Maurer et al., 2010; Stummer et al., 2004; Wilkinson et al., 2006a, 2012). Wilkinson et al. (2006a) proposed the 'Compare R (CR)' method to automatically generate a set of optimized arrays that maximize the subsurface resolution for the 2-D resistivity surveys with electrodes array along a straight line on the ground surface. This algorithm is considered the most accurate approach among the techniques examined by Loke et al. (2010a). However, the shortcoming of this algorithm is the long computation time to generate the arrays. During the last decade, there were many researches that improved the original CR algorithm yielding more effective performance. With the use of matrix-matrix multiplication algorithms and the parallel processing capabilities of modern central processing units (CPUs), this shortcoming has been greatly reduced (Loke et. al, 2010a; 2010b). Hence, the fast method makes it practical to calculate the optimized arrays for longer 2-D lines and for the 3-D survey (Loke et al., 2015a). In addtion, the practical aspects improved upon by Wilkinson et al. (2012) are the minimization of electrode polarization effects and estimation of the data error to use this technique for field surveys.

The optimized array is still a relatively new area of study with few extensive studies of its performance compared to the conventional arrays. Therefore, this study provides a valuable insight into assessing the effectiveness and reliability of this new trend of resistivity measurements technique. In the 2-D resistivity survey, two sets of optimized arrays were generated and assessed which are modified compare R

optimized arrays (CR) (Wilkinson et al., 2012) and noise-weighted compare R optimized arrays (NWCR) (Wilkinson et al., 2012). The examination of the reliability and effectiveness of these optimized arrays were illustrated by comparing them with conventional arrays; Dipole-Dipole (DD), Wenner-Schlumberger (WS), and Wenner (W) in three different stages (synthetic model test, laboratory experiment, and field cases studies). Moreover, the modified CR method was extended and modified to generate a set of arrays in case of the constrained area which is 3-D optimized perimeter arrays. Four sets of optimized perimeter arrays were generated. 1- Optimized perimeter arrays (OPN6) with maximum geometric factor limit corresponding to n=6 for the DD array. 2- Optimize perimeter arrays (OPN10) with a maximum geometric factor limit corresponding to n=10 for the DD array. 3- Noise-weighted optimized perimeter arrays (NWOPN6) with maximum geometric factor limit corresponding to n=6 for the DD array and 4- Noise-weighted optimized perimeter arrays (NWOPN10) with maximum geometric factor limit corresponding to n=10 for the DD array. Therefore, the performance of these optimized perimeter arrays was illustrated and compared with standard L and Corner (LC) arrays proposed by Tejero-andrade et al. (2015) in three different stages, model resolution test, synthetic model test and field cases studies.

1.2 Problem statement

i- In 2-D resistivity survey,

The resolution, reliability and good imaging of the subsurface model depend on many aspects. One of them is the selected electrode configurations. However, there are many conventional arrays used for resistivity measurements (e.g. DD, WS and Wenner, etc.) each may suffer one or more of the following limitations; weak signal

strength, poor model resolution, limited depth of investigation, poor sensitivity to vertical and/or horizontal change, low horizontal coverage (Loke, 2016 and 2018). In general, the Wenner array has good signal strength among other arrays but it has poor resolution and limited depth of investigation. However, the WS array has weaker signal strength than Wenner array but it is stronger than DD array. Moreover, WS is moderately sensitive to both vertical and horizontal structures meanwhile DD is good for mapping vertical structure while poor to resolve horizontal structure. In this regards, the conventional resistivity arrays may not be able to retrieve the resistivity distribution with adequate accuracy, resolution, and depth of investigation, especially in the complicated subsurface structures.

ii- 3-D survey of constrained areas,

3-D resistivity tomography is commonly used to resolve complex geological structures such as Karstic structures (Loke et al., 2013; Loke, 2018). Normal 3-D surveys attempt to cover the survey area using roughly parallel lines. However, in developed and urban areas, it is not possible to use normally implanted electrodes and the geo-electrical exploration methods are challenged when applied to such highly urbanized areas. Therefore, one solution is to use a non-contact capacitively coupled resistivity meters (Kuras et al., 2006) but this kind of system is less widely available and are more expensive than conventional systems. In this regard, the practical solution and an interesting special case of a 3-D survey are to deploy the electrodes around the perimeter of the survey area. Many alternative approaches have been developed to overcome this situation (Baker et al., 2001; Argote-Espino et al., 2013; Chávez et al., 2014 and Tejero-andrade et al., 2015). However, these techniques normally used the heuristic rules and are designed for perimeters with sharp corners such as rectangles and might not be applicable for perimeters with smooth shapes such as a circle.

Therefore, with the availability of new improvements to automatically select optimized arrays that maximize the model resolution of the subsurface, the optimized perimeter arrays were described as an alternative method for such cases.

1.3 Research objectives

The main objectives of this research are:

i- In the 2-D resistivity survey,

- To examine the effectiveness of two sets of optimized arrays (NWCR and CR) based on the modified compare R method and compare their performance quantitatively with commonly used conventional arrays (DD, WS and Wenner) using synthetic models test and laboratory experiment.
- To validate the effectiveness of these arrays in detecting and mapping the near surface geophysical features utilizing three different cases studies.

ii- In the 3-D resistivity survey of the constrained area,

- To develop the optimized perimeter arrays for the special case of 3-D resistivity surveys (in constrained areas) based on a modified CR optimization method.
- To improve the resolution of 3-D resistivity surveys along the perimeter of a constrained area using noise-weighted optimized perimeter arrays.
- To evaluate the effectiveness of optimized perimeter arrays and compare their performance with the standard 'L and corner' arrays using, model resolution, synthetic models test and field cases studies.

1.4 The novelty and significance of the research

In the first part of this research, since Wilkinson et al. (2012) work have been published, there is no extensive assessment of the NWCR and CR optimized arrays

with comparing their performance with conventional arrays. Therefore, the modified compare R algorithm (Wilkinson et al., 2012) was used to generate two sets of optimized arrays. These are conducted to get the best possible 2-D resolution and the better depth of investigation whilst using almost the same number of measurements of conventional arrays. In addition, the conventional arrays (W, WS and DD) that used in this research were also modified to address the polarization effects and generated with selecting an upper limit set for the geometric factor (the same limit used for optimized arrays) to filter out the arrays that are likely to be unstable. This is done to be consistent with the optimized arrays in comparing their effectiveness.

Consequently, qualitative and quantitative (statistical) evaluations were applied in this work to assess the two sets of optimized arrays (NWCR and CR) and conventional arrays (DD, WS and Wenner) to retrieve the true resistivity values and detect the subsurface target details (size, shape, and depth).

However, the main novelty of this research lies in improving the resolution of 3-D resistivity surveys along the perimeter of a constrained area using optimized perimeter arrays. Therefore, the optimized perimeter approaches were introduced and then four optimized perimeter arrays were generated. The effectiveness of these new arrays was investigated and compared with the standard 'L and Corner' arrays that developed up to date to overcome the physical obstructions in the constrained areas.

1.5 Thesis structure

The layout of this thesis is structured as follows:

Chapter 2 contains the general principle and theory of electrical resistivity method. The section contains a brief review of available optimized arrays methods. This is including the original version of compare R algorithm and its modifications. In

addition, the brief report on the commonly used conventional arrays (DD, WS, and W) is explained. This chapter also includes a literature review of previous studies reported in the literature about the resistivity arrays for 3-D resistivity survey in a constrained area.

Chapter 3 is dedicated to the methodological framework of 2-D and 3-D optimized arrays. The research involves the generation of 2-D optimized arrays based on a modified compare R method and modified commonly used conventional arrays (DD, WS and W) in terms of minimizing the polarization effects. This chapter also contains the discussion of four synthetic models and three field case studies that will be used to evaluate the effectiveness and performance of optimized and conventional arrays. Moreover, the 3-D resistivity survey will introduce in case of the constrained area using perimeter electrodes arrays. Then, the optimized perimeter arrays are presented. The effectiveness of these optimized arrays is illustrated using four synthetic models and three field cases studies. The performance was compared with the standard 'L and corner' arrays that developed to cover the same problem in the urban area.

Chapter 4 presents the results and discussion. It starts with the results of the 2-D case, which contain the results of synthetic models test and the quantitative assessment of the results to evaluate both optimized and conventional arrays for this stage. The second section will demonstrate the results of 2-D resistivity survey in three field case studies and the performance is compared with another geophysical tool or available borehole data. In the other hand, the results of the 3-D special case are also discussed in this chapter, which contains the results, and discussion from four synthetic models for standard 'L and corner' array and four optimized perimeter arrays as

described in chapter 3. This is followed by dedicating the results in this case from three different field studies.

Lastly, Chapter 5 summarizes the significant conclusions from this research including the recommendations for further investigation and future research.

CHAPTER 2

LITERATURE REVIEW

2.1 Overview

This chapter summarizes the basic concepts of 2-D and 3-D electrical resistivity imaging, field procedures, electrodes configurations, optimized arrays methods, forward and inversion modelling. The literature relevant to the optimization arrays is also presented here.

Electrical resistivity tomography (ERT) is one of the oldest and most commonly used geophysical methods (Dahlin, 2001; Loke, 2018). Due to the broadest range of the electrical properties of the earth materials (Figure 2.1), the resistivity techniques can be more sensitive to changes in the subsurface than other geophysical methods. Therefore, this characteristic makes electrical prospecting technique played an increasingly important role in addressing a wide range of subsurface structures in many moderately complex areas (Loke, 2018; Loke et al., 2013) including, groundwater exploration (Page, 1968), salt-water intrusion (Wilson et al., 2006), hydrocarbon and mineral prospecting (Bauman, 2005; Legault et al., 2008), contamination monitoring, (Chambers et al., 2006; Dahlin et al., 2002; Reynolds, 2011; Rucker et al., 2010) and archaeological aspects studies (Gündoğdu et al., 2017; Tsokas et al., 2008). In recent times, resistivity surveying has also been broadly applied to the engineering and environmental problems (Auken et al., 2006; Benyassine et al., 2017; Dahlin, 1996; Loke et al., 2013). In the last few years, with huge developments in computerized data acquisition systems and vast improvements in the 2-D and 3-D inversion software, the resistivity imaging technique has become an increasingly attractive exploration method (Dahlin and Zhou, 2004).

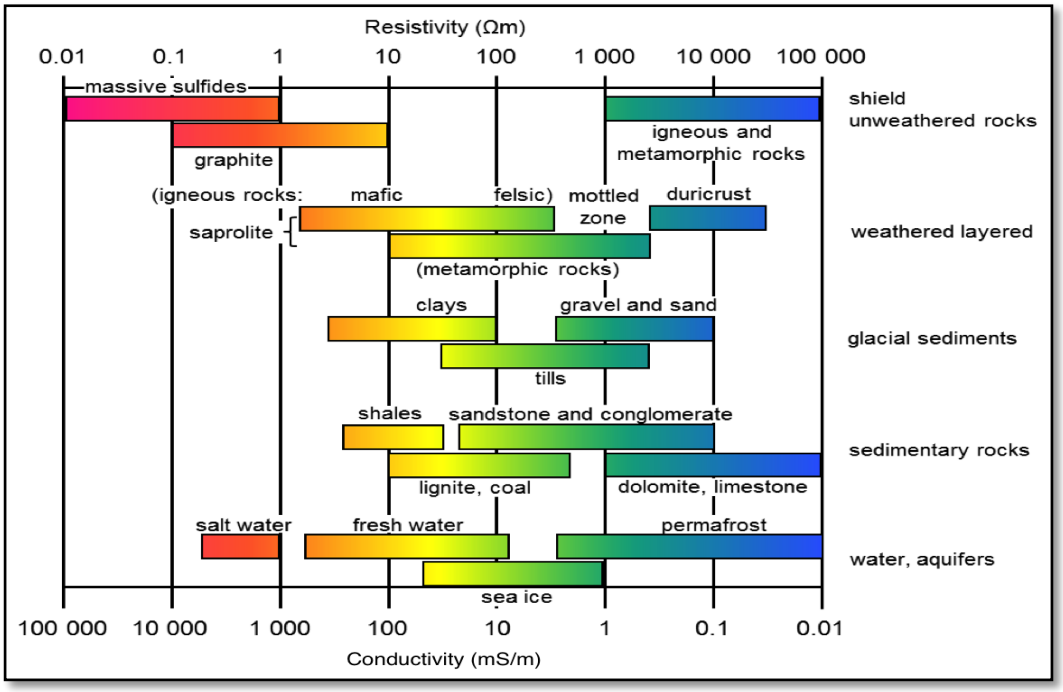

Figure 2.1: Resistivity value ranges for a common earth material and rocks (Palacky, 1988).

Up till the late 1980s, 1-D vertical electrical sounding for investigating the vertical variations and electrical profiling for assessing lateral variations were the only common techniques for conducting resistivity surveys (Loke et al., 2013; Telford et al., 1990). Within the last two decades, there have been vast improvements to the resistivity method, whereby, the 2-D and even 3-D resistivity surveys are now conducted in areas of complex structural geology. Therefore, electrical resistivity measurements are made by placing the current and potential electrodes in contact with the ground in a certain pattern that are commonly called electrode configurations (or arrays), for instance the Wenner (W), Wenner-Schlumberger (WS), Dipole-dipole (DD), Pole-dipole (PD) and Pole-pole (PP) arrays (Reynolds, 2011; Telford et al., 1990). Modern equipment (e.g. Parsekian et al., 2017) allows the generation of these arrays automatically and each has advantages and disadvantages. The effectiveness and the characteristics of these arrays in terms of the signal strength, the sensitivity of the array to horizontal and/or vertical structures, the horizontal data coverage, the

resolution and the depth of investigation were listed in Table 2.1 (Griffiths and Barker, 1993; Loke, 2018).

Table 2.1: Effectiveness of the different array types classified from A to D, representing good to poor.

Array type	Single strength	Sensitivity to horizontal structures	Sensitivity to vertical structures	Horizontal data coverage	Resolution	Depth of investigation
W	A	A	D	D	D	D
WS	B	C	C	C	C	C
DD	D	D	A	B	B	B
PD	C	C	D	B	C	B
PP	A	C	C	A	C	A

Many studies have been made on the efficiency of these arrays and by comparing them from many different aspects of model fidelity and inversion robustness (e.g. Dahlin and Zhou, 2004). Martorana et al. (2017) systematically compared some of the traditional electrode arrays in synthetic and field data using multichannel 2-D imaging system. Cubbage et al. (2017) proposed many modifications to the Wenner array to make better use of the available multichannel 2-D imaging system to improve the efficiency of this array in field data acquisition. Al-hameedawi and Thabit (2017) made a comparison between four traditional electrode arrays to examine their resolution and ability to delineating the layers in complex sedimentary deposits. Therefore, the characteristics of the different conventional arrays in terms of resolution, depth of investigation and signal to noise ratio (S/N) are well known and the researchers understand the usefulness of each array for a given target (Wilkinson et al., 2006a).

A computer-controlled resistivity meter system connected to a multi-electrode cable system automatically selects the appropriate four electrodes for each measurement to give a 2-D coverage of the subsurface. This system has enabled the

use of a large variety of arrays and survey arrangements outside of the conventional arrays listed above. The first efforts to optimize the geophysical prospection datasets were in the late of 1990s. The main aim was to obtain the optimal group of electrode arrays that would retrieve a good representation of the targets. The biomedical imaging (Isaacson, 1986) that was developed in the late of 1980s which include the adjustment of the conductivity distribution of injected currents to increase the response of a selected target, was an inspiration for Cherkaeva and Tripp (1996). They were adapting Isaacson's principles, to optimize the resistivity data sets with few electrodes for improving the reconstructions of the subsurface resistivity distribution through a selection of optimal injected currents.

Thereafter, research has highlighted the possibility of an automatically select optimal group of electrodes configurations to produce the highest subsurface image resolution. For example, the sensitivity analysis scheme (Furman et al., 2003, 2004, 2007) developed to identify electrode arrays that have the greatest sensitivity to resolve separately localized of the subsurface resistivity variations based on maximizing a sum of the Jacobian matrix elements (i.e. the sum of configuration sensitivities). The arrays that have highest sensitivities were selected as optimal arrays for resistivity imaging. On the other hand, in the object orientated focusing scheme (Hennig et al., 2008; Hennig and Weller, 2005) the required number of resistivity measurements were minimized by optimizing the sensitivity distribution of measurements in comparison to a given sensitivity distribution of the targets. This is done by analysing the weight factors obtained during object orientated focusing. The measurements that have high weights were selected while those with low weights were excluded.

Whilst, the significant progress in alternative optimized approaches for collinear surface electrode arrays were developed to enhance the ERT resolution for ground surveys based on the model resolution matrix (Loke et al., 2010a, 2014b, 2014c, 2015a; Maurer et al., 2010; Stummer et al., 2004; Wilkinson et al., 2006a, 2012). Recently, there are four different optimization algorithms to generate a set of electrodes arrays. These methods based on maximizing the sum of the model resolution elements named "Eidgenossische Technische Hochschule" (ETH) (Stummer et al., 2004), British Geological Survey method (BGS) (Wilkinson et al., 2006a), Compare R method (Wilkinson et al., 2006a), and Combined BGS-CR method (Loke et al., 2010a).

Stummer et al. (2004) pioneered and developed the real-time experimental design approach, which called Eidgenossische Technische Hochschule (ETH) or Goodness Function (GF) method. This method implemented the first power of the sensitivity distributions to compute approximations of the model resolution matrix. It starts by using an initial small dataset such as conventional DD arrays. Then, selected electrodes configurations were added to the initial datasets based on their effectiveness on the model resolution matrix. The configurations were ranked based on the goodness function (GF) that assesses the effects of its addition to the base set and based on how well they maximized the model resolution. Arrays that improved the model resolution were selected while those that reduced the model resolution were excluded. Szalai et al. (2013) tested and compared the optimized Stummer configurations with many conventional arrays. They conclude that the optimized Stummer arrays have a better resolution than conventional arrays.

Wilkinson et al. (2006a) have proposed a modified GF (MGF) method and a new method of compare R (CR). The modified GF method (MGF) also called the BGS

method. It uses the second power of the sensitivity value to calculate approximations of model resolution whereas the new method 'compare R' (CR) recalculate the model resolution (R) directly for each added-on configuration and its considered the best method to maximize the model resolution but it took longest computation time. This compare R method has subjected to several modifications (Loke et al., 2010a, 2010b, 2014b, 2015b; Wilkinson et al., 2012). Later in this chapter, this compare R optimization method and its modifications will be discussed in some details.

Loke et al. (2010a) have combined the BGS and CR methods that proposed by Wilkinson et al. (2006a) to get their best features to select the set of arrays configurations that will give the maximum amount of information about the subsurface and of fast computation.

Alfouzan et al. (2010) extensively evaluate these four optimization strategies in comparison with conventional arrays in terms of model resolution calculation, synthetic models and field surveys to maximize the amount of information regarding a subsurface with 2-D electrical imaging surveys. They conclude that the results from the optimization methods have better resolution and identify accurate information than conventional arrays. Then after, with the advancements in Compare R algorithms (Loke et al., 2010a, 2010b; Wilkinson et al., 2012), the practical application of the optimized array has now been feasible. For example, array optimization for cross-borehole surveys (Loke et al., 2014b), 3-D surveys (Loke et al., 2014c), long 2-D survey lines (Loke et al., 2015b) and combined surface with buried electrodes (Loke et al., 2015a).

2.2 The basic theory of the resistivity method

The comprehensive theory of the resistivity method is given in many textbooks such as (Reynolds, 2011; Telford et al., 1990). Generally, ERT investigations assumed the earth acts as a linear conductor and the theory used in the resistivity method is based on the Ohm's law, that governs the relationship between the intensity of the electrical field, *E* (volts per meter), and current density, *J* (Amps per unit area). The simple form of Ohm's law for current flow in a continuous medium is stated as follow:

$$J = \sigma E \tag{2.1}$$

where σ is the electrical conductivity of the medium (mho per m).

In an isotropic medium, the conductivity will be a scalar quantity and so that the current density (J) and the magnitude of the electrical field (E) will be in the same direction. Following Maxwell's equations of the stationary case, the electric field intensity (*E*) is the negative gradient of the electric potential (ϕ) and the relationship is given in equation (2.2):

$$E = -\nabla\phi \tag{2.2}$$

Here, E is the gradient of a scalar potential, ϕ in volts. By substituting the equation (2.2) into the Ohm's law in equation (2.1) to find:

$$J = -\sigma\nabla\phi \tag{2.3}$$

Hence, by taking the divergence of the current density one can obtain:

$$\nabla . J = -\nabla . (\sigma\nabla\phi) = 0 \tag{2.4}$$

Since σ is a constant equation 2.4 reduces to

$$\nabla^2\phi = 0 \tag{2.5}$$

This is the Laplace's equation, where ∇^2 is a second derivative operator and ∅ is the potential. To solve this equation and find the potential, two boundary conditions

must be satisfied which are, the potential must be continuous across the boundary and the normal component of the current density must be also continuous.

Consider the simplest case, where a homogeneous subsurface and a single point current electrode C_1 at the Earth's surface and the second current electrode C_2 at infinity (Figure 2.2) and its effect is neglected. In this case, the current flows radially away from the source and it is perpendicular to the equipotential surface, which has a hemisphere shape. The potential is a function of distance (r) from the current electrode. Then, the equation (2.5) is applicable due to the potential has spherical symmetry in the earth and the potential will be a function of the radial distance (r) from the current electrode only. Then can be simplified in spherical coordinates into this equation (2.6)

$$\nabla^2\phi = \frac{d^2\phi}{dr^2} + \left(\frac{2}{r}\right)\frac{d\phi}{dr} = 0 \qquad (2.6)$$

To solve the above equation, multiply it by r^2 and integrating, then this equation was obtained equation (2.7)

$$\frac{d\phi}{dr} = \frac{A}{r^2} \qquad (2.7)$$

Then integrating equation 2.7 again to get equation (2.8)

$$\phi = -\frac{A}{r} + B \qquad (2.8)$$

A and B are constant. From this equation, when r goes to infinity, it is reasonable the potential (ϕ) equal to zero and this gives the value of B = 0. The current flows radially away from the source and it is perpendicular to the equipotential surface, which has a hemisphere shape. Thus, the total current crossing the hemisphere with an area equal to $\frac{1}{2}(4\pi r^2)$ is given by the following formula:

$$I = 2\pi r^2 J \qquad (2.9)$$

Substituting *J* from equation (2.3) into (2.9) to reach to the following form:

$$I = -2\pi r^2 \sigma \frac{d\phi}{dr} \quad and\ then, \qquad I = -2\pi\sigma A \tag{2.10}$$

Hence, rewritten and rearranging (2.10) to this form (2.11):

$$A = -\frac{I\rho}{2\pi} \tag{2.11}$$

Consequently, from equation (2.8), one can obtain this solution of the potential in the case illustrated in Figure (2.2):

$$\phi = \frac{I\rho}{2\pi r} \tag{2.12}$$

Then rearrange (2.12) to get apparent resistivity as follow:

$$\rho = \frac{2\pi r\phi}{I} \tag{2.13}$$

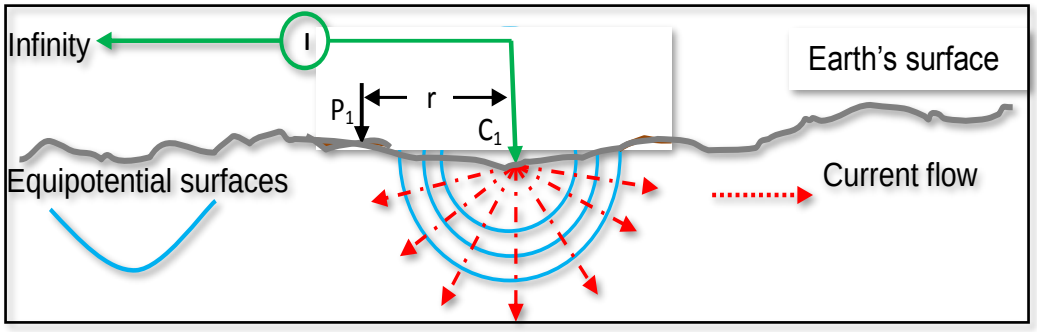

Figure 2.2: The flow of current from a point current source (the second electrode at infinity) and the resulting equipotential distribution.

However, in practice, all resistivity surveys use at least two current electrodes in which the distance between them is finite and one of them is a positive current while the other one is a negative current source. The potential distribution caused by two-point currents electrodes have a symmetrical pattern about the vertical place at the mid-point between them and is shown in Figure (2.3). Both current electrodes will

affect the potential at any point in the surface and the potential value due to the C1 at P1 is:

$$\phi_1 = -\frac{A_1}{r_{c_1}} \qquad (2.14)$$

In addition, the potential due to C_2 at P_1 is:

$$\phi_2 = -\frac{A_2}{r_{c_2}} \qquad (2.15)$$

Since, $A_1 = -A_2 = A$, Therefore:

$$\phi_1 + \phi_2 = \frac{I\rho}{2\pi r_{c_1}} + \left(-\frac{I\rho}{2\pi r_{c_2}}\right) \quad then, \qquad \phi = \frac{I\rho}{2\pi}\left(\frac{1}{r_{c_1}} - \frac{1}{r_{c_2}}\right) \qquad (2.16)$$

Where r_{C_1} and r_{C_2} are distances of the point from the first and second current electrodes. However, in all surveys, the potential difference between two points is measured. The electrode configuration is referred to as a general four-electrode configuration as shown in Figure (2.4) and the potential difference is then given by:

$$\Delta\phi = \frac{\rho I}{2\pi}\left(\frac{1}{r_{c_1p_1}} - \frac{1}{r_{c_2p_1}} - \frac{1}{r_{c_1p_2}} + \frac{1}{r_{c_2p_2}}\right) \qquad (2.17)$$

The above equation (2.17) gives the potential difference between the two potential electrodes over a homogeneous half space medium.

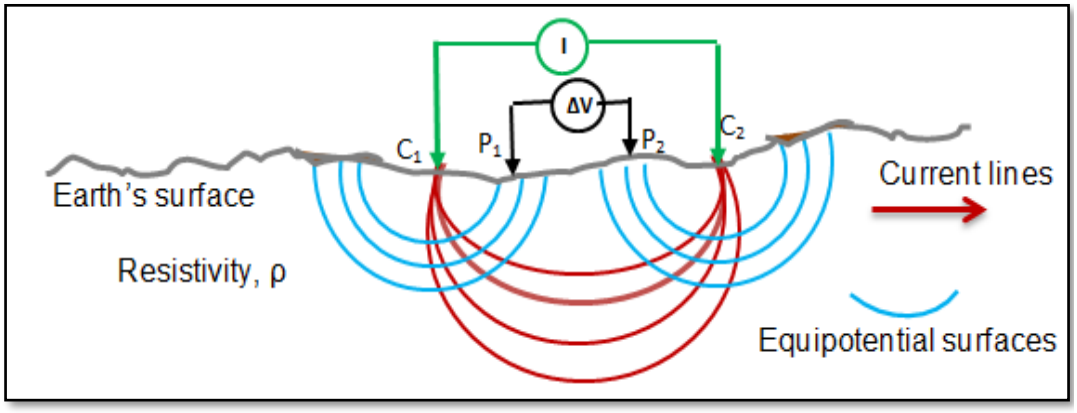

Figure 2.3: The current lines and the equipotential surfaces for two-point source electrodes.

In fact, the resistivity surveys are conducted over an inhomogeneous medium, the current distributed in 3-D directions, and the resistivity has a 3-D distribution. The resistivity survey carried out using four electrodes planted in the ground surface (Figure 2.4). Two of them are injecting current (electrodes C1 and C2) while the two other electrodes are measuring the resulting potential difference, (P1 and P2) Figure (2.4). Then, from the current (I) and potential difference ($\Delta\phi$), the resistivity value is calculated using equation (2.18), which called apparent resistivity (ρ_a) because of the measured resistivity is usually a composite of the resistivity of several layers (heterogeneous earth):

$$\rho_a = \frac{\Delta\phi}{I} \frac{2\pi}{\left(\frac{1}{r_{c_1p_1}} - \frac{1}{r_{c_2p_1}} - \frac{1}{r_{c_1p_2}} + \frac{1}{r_{c_2p_2}}\right)} \qquad (2.18)$$

Where,

$$K = \frac{2\pi}{\left(\frac{1}{r_{c1p1}} - \frac{1}{r_{c2p1}} - \frac{1}{r_{c1p2}} + \frac{1}{r_{c2p2}}\right)}$$

k is a geometric factor that depends on the arrangement of the four electrodes and then:

$$\rho_a = K \frac{\Delta\phi}{I} \qquad (2.19)$$

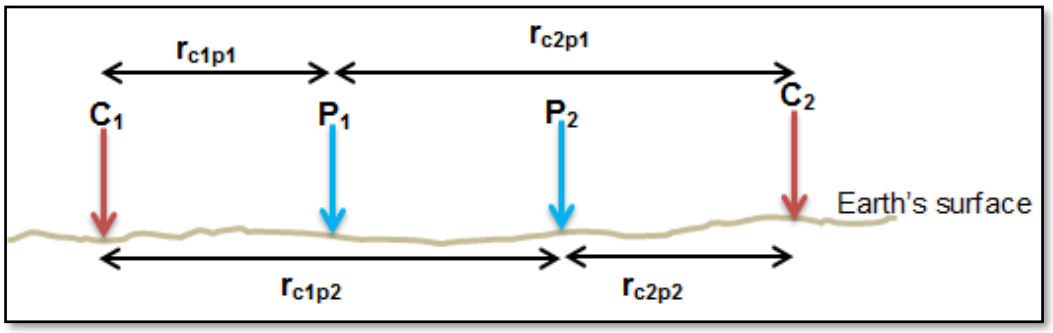

Figure 2.4: General four electrodes configuration for measuring resistivity.

Transforming a set of apparent resistivity data into the true resistivity distribution of the subsurface is the fundamental challenge for interpretation techniques.

The relationship between the measured “apparent” resistivity and the “true” resistivity is an intricate relationship. Inversion programs generate the true subsurface resistivity from the apparent resistivity values. Resistivity is a physical property of rocks and minerals that show the broad rang variation (Figure 2.1). Rocks and minerals are considered good, intermediate, or poor conductors based on many parameters such among, containing minerals, the porosity of the rock, water saturation, and water salinity and so on.

2.3 2-D Resistivity surveys

The change in the resistivity distribution laterally and vertically in the subsurface can be measured using a 2-D resistivity imaging survey. Resistivity surveys primarily measured using a four-electrode system (i.e. current electrode pairs and potential electrode pairs). However, modern 2-D acquisition system utilizes the 2-D multi-electrode cable system and can use more than 25 to 100 electrodes connected along survey lines with multi-core cables (Loke et al., 2013) which in turn is connected to the resistivity meter (Figure 2.5). This system reduces the time of field data acquisition. Many electrode configurations can be applied to a multi-electrode survey line with a range of different geometries. The electrode sequence address files (Protocols) are uploaded from a personal computer (PC) onto the resistivity meter. A sequence address file contains a list of configurations instructing the instrument to apply an electrical current and measure potential difference according to the electrode array geometry used for a given number of electrodes.

The spacing between electrodes must be fixed throughout the survey line, which arranged according to the required resolution and depth of investigation, while the distance between current and potential electrodes depends on electrode configuration. This distance is controlled automatically by resistivity meter according to the uploaded protocol. The whole array is then gradually moved along the profile and the resistivity meter sequentially records one resistivity measurement in each step. The all measured data from the first electrode inter-spacing form the first data level. Then after, the spacing between electrodes is increased and a second data level is measured. This process is repeated until the maximum spacing between the electrodes is reached (Figure 2.5). The data then plotted in a 2-D pseudo-section, which represents the vertical and lateral resistivity distribution (Edwards, 1977; Loke, 2018).

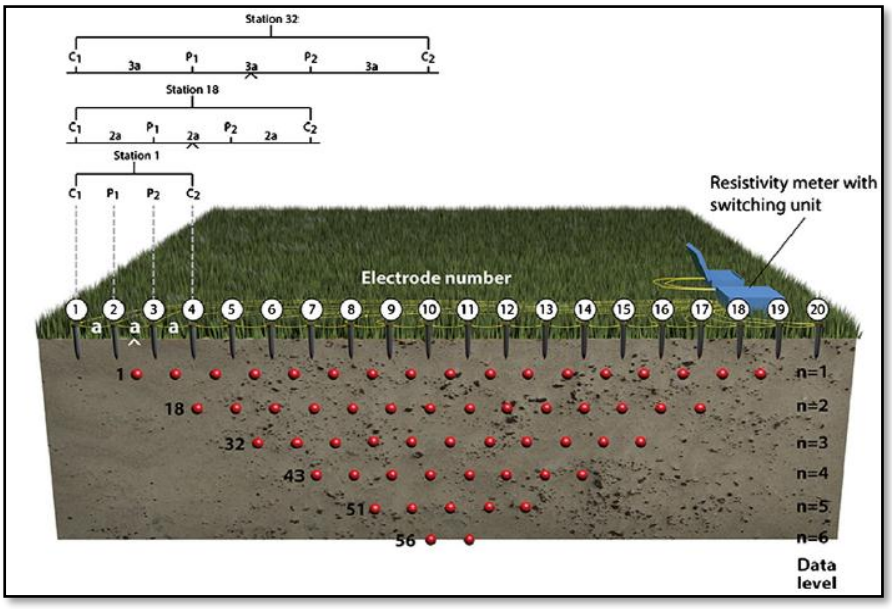

Figure 2.5: Diagram shows a multi-electrode system and measurements levels to build up a 2-D pseudo-section. (From British Geological Survey, Natural Environment Research Council 2013, Loke et al., 2013).

In principle, resistivity measurements can be made with any configuration of the four electrodes. With the deployment of a large number of surface electrodes in a line over the targeted area and the use of multichannel receivers, a large number of

measurements can be collected efficiently. Direct current or low frequency alternating currents (less than10 Hz) are injected into the ground through a pair of point electrodes (C_1 and C_2) and measuring the potential differences arising between another pair of electrodes (P_1 and P_2). The resulting potential differences provide information about the subsurface resistivity distribution. The current and potential electrodes are to be arranged in a certain pattern that is commonly called electrode configurations or arrays. The most commonly used conventinal arrays are described and illustrated in Figure (2.6) including of, Wenner (W), Wenner-Schlumberger (WS), and Dipole-Dipole (DD) (Loke et al., 2013; Reynolds, 2011; Telford et al., 1990). However, recently there is a new trend to collect resistivity data based on a maximized model resolution which called optimized arrays. In the following subsuctions, the more common conventional arryas (W, WS, and DD) and optimized compare R (CR) algorithms are briefly discussed.

2.3.1 Common conventional arrays

The main characteristic of electrode configurations is its geometric factor which related to the electrode arrangement and spacing (refer to Eq. (2.18)). Each of commonly used conventional arrays that discribed in Figure (2.6) has different characteristics such as, signal strength, lateral and vertical sensitivities, horizontal caverage and depth of investigation. Hence, each of them has different performances and capabilities regarding resolve the different geological features of the survey area and the quality of measured data is affected by the choice of electrode configuration (Loke et al., 2013). Although the availability of automated systems that use to acquire more flexible electrode configurations, many conventional arrays still frequently used.

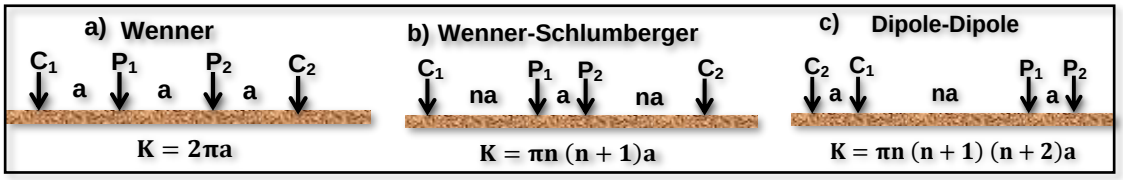

Figure 2.6: Common arrays used in resistivity surveys a) W, b) WS and c) DD, with their geometric factors after.

2.3.1(a) Wenner (W) array

The Wenner array is the simplest, popular and widely used electrode configuration among the researchers because of it requires much smaller data than the others to build-up a pseudo-section and then the acquisition time is short (Barker et al., 2001). The four electrodes (the outer electrodes are the current electrodes C_1 and C_2 while the two inner electrodes are potential electrodes P_1 and P_2) are arranged collinearly with equally spaced from each other as shown in Figure (2.6a) (Loke, 2018). This array has the strongest signal strength due to it has a smaller geometric factor which is a significant parameter for survey areas that have high background noises. Most of the early resistivity surveys using 2-D multi-electrode system were conducted with Wenner array (Loke, 2018).

This array has high sensitivity to the vertical changes of the resistivity distribution under the center of the array. However, it is relatively less sensitive to the horizontal variations of the subsurface resistivity distribution. Therefore, it is the best to detect the horizontal subsurface structures and is relatively poor in resolving the vertical structures (Loke, 2018).

There are three possible combinations of electrode configurations represented this type of array. The Wenner-Alpha array is the standard Wenner array (Figure 2.6a). The other two combinations of Wenner arrays are Wenner-Beta and Wenner-Gama configurations. Beta type is considered a case of Dipole-Dipole array while in the

Gamma type the current and potential electrodes are interchanged (Carpenter and Habberjam, 1956).

2.3.1(b) Wenner-Schlumberger (WS) array

This array is a crossbreed between Wenner array and Schlumberger array (Loke, 2018; Pazdirek and Blaha, 1996). In this array (Figure 2.6b) the electrodes are arranging with constant spacing "a" between potential electrodes P_1 and P_2, and the spacing "na" that increases logarithmically. The ratio of the distance between C_1 and P_1 or (C_2-P_2) and the distance between potential electrodes (P_1-P_2) is called "**n**" factor. Therefore, the geometric factor of this array depends on this "**n**" factor and "a" electrode spacing. The signal strength of WS array is smaller than the Wenner array but it is stronger than DD array. In addition, this array is reasonably sensitive to both vertical and horizontal structures. This is because, WS array is moderately sensitive to both vertical and lateral changes in the subsurface resistivity distribution. Therefore, it is a good choice where the vertical and horizontal geological structures are expected. In term of horizontal coverage, WS array has a slightly wider coverage compared with the Wenner array but the horizontal data coverage is slightly narrower than the DD array.

2.3.1(c) Dipole-Dipole (DD) array

In this array (Figure 2.6c), both potential electrodes (P_1 and P_2) are on the outside of the current electrodes C_1 and C_2. The spacing between each of electrodes pair has a constant spacing "a" and the spacing between the innermost pair is "**na**" and it is always equal to or greater than "a" spacing. DD array has a maximum sensitivity for resistivity changes between both current electrodes pair and potential electrodes